

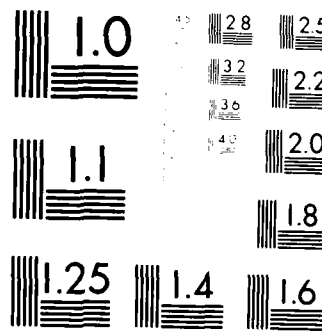
AD-A152 090 PLASTIC DEFORMATION OF CRYSTALLINE POLYMERS(U) AKRON 1/1  
UNIV OH INST OF POLYMER SCIENCE R N GENT ET AL. MAR 85  
TR-36-15 N60014-76-C-0488

UNCLASSIFIED

F/G 11/9

NL

END  
IN UNCL  
DTIC



MICROCOPY RESOLUTION TEST CHART  
NATIONAL BUREAU OF STANDARDS

(2) H

AD-A152 090

OFFICE OF NAVAL RESEARCH

Contract N00014-76-C-0408

Project NR 092-555

Technical Report No. 36

PLASTIC DEFORMATION OF CRYSTALLINE POLYMERS

by

A. N. Gent and Jongkoo Jeong

Institute of Polymer Science  
The University of Akron  
Akron, Ohio 44325

DTIC  
ELECTED  
S APR 8 1985 D  
B

March, 1985

Reproduction in whole or in part is permitted for  
any purpose of the United States Government

Approved for Public Release; Distribution Unrestricted

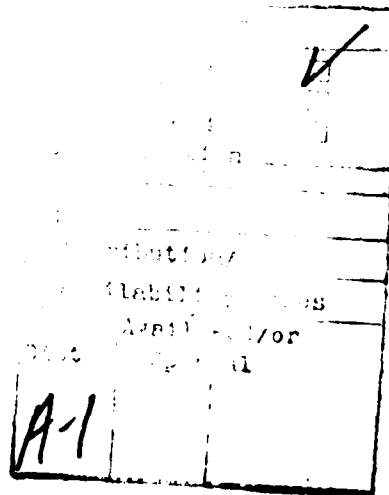
DTIC FILE COPY

85 03 21 165

SECURITY CLASSIFICATION OF THIS PAGE (When Data Entered)

REPORT DOCUMENTATION PAGE		READ INSTRUCTIONS BEFORE COMPLETING FORM
1. REPORT NUMBER Technical Report No. 36	2 GOVT ACCESSION NO. <i>A152090</i>	3. RECIPIENT'S CATALOG NUMBER
4. TITLE (and Subtitle) Plastic Deformation of Crystalline Polymers	5. TYPE OF REPORT & PERIOD COVERED Technical Report	
7. AUTHOR(s) A. N. Gent and Jongkoo Jeong	6. PERFORMING ORG. REPORT NUMBER	
9. PERFORMING ORGANIZATION NAME AND ADDRESS Institute of Polymer Science The University of Akron Akron, Ohio 44325	10. PROGRAM ELEMENT, PROJECT, TASK AREA & WORK UNIT NUMBERS NR 092-555	
11. CONTROLLING OFFICE NAME AND ADDRESS Office of Naval Research Power Program Arlington, VA 22217	12. REPORT DATE March, 1985	
14. MONITORING AGENCY NAME & ADDRESS (if different from Controlling Office)	13. NUMBER OF PAGES 31	
15. SECURITY CLASS. (of this report) Unclassified		
15a. DECLASSIFICATION/DOWNGRADING SCHEDULE		
16. DISTRIBUTION STATEMENT (of this Report) According to attached distribution list. Approved for public release; distribution unrestricted.		
17. DISTRIBUTION STATEMENT (of the abstract entered in Block 20, if different from Report)		
18. SUPPLEMENTARY NOTES Submitted for publication in: Polymer Engineering and Science		
19. KEY WORDS (Continue on reverse side if necessary and identify by block number) Crystalline polymers, Deformation, Drawing, Ductility, Plastic deformation, Polyethylene, Polymers.		
20. ABSTRACT (Continue on reverse side if necessary and identify by block number) Draw ratios have been measured for samples of polyethylene and trans-polyisoprene, crystallized at various temperatures and at various degrees of orientation. The values obtained range from unity, i.e., no drawing is observed, up to values of about 15X for materials crystallized in the oriented state and then drawn in a perpendicular direction. The results are in rough accord with a simple molecular network model in		

which network strands are incorporated into crystallites with a number of reversals of direction (folds), and the remainder of a strand between network junctions is randomly arranged. The reduction in draw ratio with increasing temperature of crystallization and with increasing orientation at the time of crystallization is then accounted for in terms of a reduction in the number of reversals (folds) per molecular strand. Differences in natural draw ratio for different polymers are attributed to variations in characteristic sequence length within a crystallite and in the number of folds per network strand.



S/N 0102-LF-014-6601

Unclassified

## 1. Introduction

One of the most remarkable features of partially-crystalline polymers is their ability to undergo large plastic deformations ("drawing") without rupture. This phenomenon is readily distinguished from plastic yielding in ductile metals, which is considerably smaller in extent, or in glassy polymers, where yielding is localized within narrow shear bands. In contrast, plastic yielding in partially-crystalline polymers takes place in a relatively homogeneous way and results in deformations of several hundred percent without rupture(1). The material then strain hardens after drawing so that further deformation is only achieved by imposing higher stresses.

Representative relations between tensile stress and displacement of the clamps securing a tensile specimen are shown in Figures 1 and 2. After the yield stress  $\sigma_y$  is reached the specimen spontaneously thins over part of its length to form a "neck" where the extension is large. The rest of the specimen is still lightly stretched. Further displacement of the clamps is achieved by an increase in the amount of material in the neck at the expense of the lightly-strained material on either side of it. This transformation continues at a constant stress, generally smaller than  $\sigma_y$ , until the whole specimen has become uniformly stretched to the "natural draw ratio", i.e., the stretch ratio set up in the neck, denoted here d.

The natural draw ratio, as discussed in more detail later, is quite different for different polymers. For example, low-density polyethylene (LDPE) can only be drawn to about 5 times its original length whereas high-density polyethylene (HDPE) can be drawn 10X - 12X. Moreover, the draw ratio depends to a considerable degree upon the conditions under which crystallization took place, being much smaller for polymers crystallized in an oriented state.

Although considerable attention has been given to the molecular structure of semi-crystalline polymers and the rearrangements that accompany plastic yielding and drawing (2,3), relatively little work has been published on quantitative aspects of the drawing process. Some preliminary observations are therefore reported here of the extent of plastic deformation that various crystalline polymers will undergo, and of the effect of the mode of crystallization upon their subsequent deformability. An attempt is then made to account for the marked differences observed in deformability between different polymers, and between different crystallization conditions for the same polymer, in terms of a simple model of the drawing process.

## 2. Experimental Details

### (i) Materials

Samples were prepared in the form of molded sheets about 2 mm thick from several materials: trans-polyisoprene (TPI), supplied by Polysar Limited, denoted TP-301; high-density polyethylene (HDPE-1), supplied by Asahi-Kasei Industries, denoted Microsuntec R340P; a second sample of molding-grade high-density polyethylene (HDPE-2) supplied by Union Carbide Corporation, denoted 8908; a sample of pipe-grade medium-density polyethylene (MDPE) supplied by Union Carbide Corporation, denoted E608; and a sample of film-grade low-density polyethylene (LDPE), also supplied by Union Carbide Corporation and denoted DFDY 0774. Trans-polyisoprene (TPI) was also examined in the lightly-crosslinked state, brought about by adding 1 percent by weight of dicumyl peroxide and 1 percent of an antioxidant (Antioxidant 2246, American Cyanamid Company) to the material before hot-pressing for 1 h at 150°C. The crosslinked material is denoted TPI-X.

Samples of HDPE-1 and TPI-X were crystallized in the oriented state by melting the molded sheets at 160°C and 95°C, respectively, for 15 minutes and then rapidly stretching them to a predetermined length. They were then cooled rapidly in the stretched state so that crystallization

took place completely before release. The exact state of orientation was determined from the dimensions of an inked grid applied to the molded sheet initially.

Measured values of the density  $\underline{d}$  of the crystallized sheets and values of the degree of crystallinity  $\underline{C}$  calculated from them are given in Table 1. No significant changes in  $\underline{d}$  and hence  $\underline{C}$  were observed with the extent of orientation imposed during crystallization.

### (ii) Determination of draw ratio

When a specimen deforms by cold drawing, the extension becomes highly non-uniform until the whole sample has been transformed into the drawn state. Further deformation then occurs homogeneously under increasing stress up to the point of rupture. The natural draw ratio is that set up in the necked region before the onset of strain hardening and subsequent uniform deformation. It was measured by the separation of grid lines placed on the sample initially. The measurements were made while the samples were under tension and in the process of being drawn.

Typical tensile stress-strain relations are shown in Figures 1 and 2 for oriented test pieces of HDPE-1 and TPI-X, stretched at a nominal strain rate of  $0.05 \text{ s}^{-1}$  at  $25^\circ\text{C}$ . When the stretching direction was at right angles to the direction of prior orientation, represented by an extension

ratio  $\lambda$ , then the corresponding value of extension ratio in the direction of extension, given by  $\lambda^{-\frac{1}{2}}$ , was less than unity. Values of the extension ratio in the direction of subsequent stretching have been employed in Figures 1 and 2 to characterize the degree of prior orientation imposed during crystallization.

### 3. Experimental Results

#### (i) Stress-strain relations

Necking and drawing took place when the prior orientation ratio  $\lambda$  was less than about 8 for HDPE-1 and less than about 2 for TPI-X, Figures 1 and 2. For greater amounts of prior orientation a distinctly different type of deformation occurred. No signs of necking were observed and, instead of a pronounced drop in tensile load at the yield point, only a change in slope of the load-displacement relation was noted, Figures 1 and 2.

Measured values of the yield stress  $\sigma_y$  are plotted in Figure 3 against the pre-orientation ratio  $\lambda$ . For HDPE-1 they did not change significantly over the entire range of orientation, being about 24 MPa, and for TPI-X only a slight increase was found, from about 9 to 14 MPa, as the degree of prior orientation increased. The difference in  $\sigma_y$  between the two

polymers may be due largely to the different levels of crystallinity; 65 percent and 36 percent, respectively. Changes in crystallite orientation or microstructure brought about by prior orientation appear to have little effect on the yield stress.

(ii) Draw ratio: Unoriented samples

Values of the natural draw ratio  $\lambda_d$  for unoriented samples of all of the materials examined are given in Table 1. They range from 2.6 for TPI-X to 12 for HDPE-2. Surprisingly, they are consistently larger for the more highly-crystalline materials, whereas one might well have expected the reverse: a greater ductility for less-crystalline materials. Moreover, the largest values are somewhat larger than one would expect for the maximum extensibility of polymer chains in a loose molecular network: rubbery materials will undergo extensions of only up to about 10X at the most, before rupture. As the present materials appear to recover completely on melting, there is no indication of molecular flow during drawing. The molecules thus appear to be retained within a network of entanglements as if they were lightly crosslinked. The high extensibility of HDPE-2 during drawing is therefore quite

surprising, particularly in view of its high degree of crystallinity. A possible model of the drawing process that accounts for these features is advanced in a later section.

(iii) Draw ratio: effect of prior orientation

Values of the draw ratio  $\lambda_d$  for oriented samples of TPI-X and HDPE-1 are plotted in Figure 4 against the prior orientation ratio  $\lambda$ , using logarithmic scales for both axes. As the degree of prior orientation was increased, so the draw ratio decreased, becoming unity; i.e., no drawing took place; when the prior orientation ratio was about 2.4 for TPI-X and about 10 for HDPE-1. On the other hand, when extension was imposed in a direction perpendicular to the prior orientation, i.e.,  $\lambda < 1$ , then the draw ratio increased, reaching values of about 4 for TPI-X and about 14 for HDPE-1.

The variation of  $\lambda_d$  with prior orientation ratio  $\lambda$  was found to be approximately an inverse proportionality:

$\lambda_d = \text{constant}/\lambda$ . The broken lines in Figure 4 are drawn with a slope of -1, consistent with this relationship. They are seen to describe the experimental results reasonably well, except in the low-orientation region when  $\lambda$  is close to unity. A dependence of this form would arise from the limited extensibility of polymer molecules, because prior orientation by a factor  $\lambda$  would reduce the additional extension ratio  $\lambda_d$  that molecular chains could undergo

before reaching the fully-stretched state, by the factor  $\frac{1}{\gamma}$ . A treatment of the drawing process in terms of the maximum possible extensibility of polymer molecules is given in the following section.

#### 4. Theoretical Considerations

A simple molecular model of the process of cold drawing in partially-crystalline polymers is now put forward. A representative molecular chain between attachment points to the network, i.e., between molecular entanglements or crosslinks, is shown in Figure 5. It consists of  $n$  freely-jointed units, each of length  $a$ , so that its fully-stretched length  $L_m$  is given by  $na$  and its mean end-to-end length  $L_o$  in the molten state, Figure 5a, is given by  $n^{1/2}a$ . On crystallization the center part of the molecule is assumed to enter a crystallite of length  $L_c$  and fold back on itself to enter the same crystallite a number of times, denoted  $f$ , Figure 5b. In order for the ends of the molecule, where it is joined to other molecules in the network, to be located on either side of the crystallite, only odd values of  $f$  are considered here. In this simple model the degree of crystallization  $C$  is given by

$$C = fL_c/L_m \quad (1)$$

It is now assumed that drawing takes place when the molecular chains entering a crystallite apply a sufficiently high stress to it so that it becomes disrupted and transforms into a new extended form, Figure 5c. A further assumption is made that the requisite stress is relatively high so that the molecules are almost fully extended at the onset of crystal rearrangement, and subsequently. Thus, the natural draw ratio  $d$  is given by

$$d = L_x / L, \quad (2)$$

where  $L$  is the end-to-end distance for a representative chain in the unoriented partially-crystalline state, Figure 5b. This is not necessarily the same as the corresponding distance  $L_0$  in the molten state, Figure 5a. Indeed, it is hypothesized that the process of crystallization will alter the distribution of chain end-to-end distances,  $L_0 \rightarrow L$ , by excluding junction points from the crystal lattice. In particular, those chains which become fully-extended first on stretching and thus initiate the disruption of crystallites will be those with junction points disposed in the direction of stretching and on either side of a crystallite, as shown schematically in Figure 5b.

An estimate of the initial junction separation distance  $L$  can be made as follows. The distance  $L$  is composed of a

crystalline sequence length  $L_c$  and an amorphous distance  $L_a$ , given approximately by the random-coil value  $L_a = \frac{1}{(1-\epsilon)^{1/2}} n^{1/2} a$ .

Hence,

$$L = L_c + L_a = (CL_m/f) + (1-\epsilon)^{1/2} L_m/n^{1/2}, \quad (3)$$

on substituting for  $L_c$  in terms of  $L_m$  from equation (1).

Thus, the natural draw ratio  $\lambda_d$  is given by

$$1/\lambda_d = (\epsilon/f) + (1-\epsilon)^{1/2}/n^{1/2}, \quad (4)$$

from equations 2 and 3.

This simple treatment suggests that the natural draw ratio will be large for materials in which the molecules re-enter the crystallites many times and  $f$  is large, even when the degree of crystallization is high. In other circumstances, the predicted draw ratio is small. Two extreme cases are now considered. In each case the number  $n$  of random links per molecular strand is given the representative value, 200.

For TPI-X, the degree of crystallinity  $\epsilon$  is 36 percent and the natural draw ratio is about 2.6, Table 1. From equation 4, the average number of times  $f$  that a chain passes through a crystallite is obtained as 1.1, indicating that for this material there is relatively little re-entry or chain-folding. For HDPE-2, on the other hand, the degree of crystallinity is 72 percent and the natural draw ratio is about 12. From equation 4 the average number of times  $f$

that a molecular chain passes through a single crystallite is obtained as 15.6, indicating that there is a great deal of re-entry or folded-chain crystallization in HDPE-2, as prepared here.

From the number of random links involved in crystalline sequences, 72 for TPI-X and 144 for HDPE-2, and the inferred number of times that each chain enters the same crystallite, we may deduce the mean length  $\bar{L}_c$  of a crystallite to be 65 random links for TPI-X and 9.2 random links for HDPE-2. The latter number is consistent with the known crystal microstructure of polyethylene, corresponding to about 5-10 nm, but the value for TPI-X seems unacceptably high. It should be noted, however, that the present analysis does not distinguish between a chain passing through a single crystalline sequence in the direction of stretching or a chain passing through two or more crystalline sequences, without reversing direction, before a junction point is reached. Thus, the large number of random links deduced for the crystalline sequence length in TPI-X may in reality be the sum of several crystallite lengths traversed by the same molecular strand. Nevertheless, a clear implication of the present analysis is that chain-folding is much less prominent in TPI-X and that the crystallites are considerably longer (thicker) than in HDPE. It would be interesting and worthwhile to examine other partially-

crystalline polymers and to make direct comparison with their crystallite thicknesses, determined, for example, by SAXS.

The large effect of prior orientation upon the draw ratio  $\lambda_d$ , discussed previously and shown in Figure 4, can be interpreted in terms of the molecular model advanced here. It is in accord with a continuous change in the chain end -to-end length  $L$  with prior orientation, as might well be expected, with a corresponding reduction in the number of times that a molecular strand traverses a single crystallite.

##### 5. Effect of Annealing or Quenching

A direct implication of the analysis given here is that an increase in crystallite thickness, brought about by annealing, for example, should result in fewer re-entries and a decrease in the natural draw ratio. Conversely, a decrease in crystallite thickness and corresponding increase in number of molecular re-entries should cause an increase in natural draw ratio. Unoriented samples of HDPE-1 and TPI-X were therefore prepared by melting sheets and allowing them to crystallize at different temperatures so that the crystallite layer thicknesses would be somewhat different. Values of the natural draw ratio are given in Table 2. As can be seen, the higher the temperature  $T_c$  of crystallization (and, hence, the thicker the crystallite), the lower  $\lambda$  the natural draw ratio  $\lambda_d$ , in general. This trend is in accord with the mechanism of cold drawing put forward here.

## 6. Conclusions

Measurements have been made of the tensile properties of several representative partially-crystalline polymers, crystallized both in the oriented and unoriented state. The yield stress was found to be virtually unchanged by prior orientation but the natural draw ratio decreased in inverse proportion to the amount of preorientation.

Striking differences were found between the natural draw ratio for various polymers. A simple molecular model for the drawing process was developed in terms of a loose network of molecules, held together by entanglements or crosslinks which are excluded from the crystal lattice. As a result, the end-to-end distance for molecular strands in the partially-crystalline material is different from that in the melt. Under tension, certain strands become fully-stretched and initiate disruption of the crystallites, followed by their rearrangement into the fully-drawn state. The principal term in the analysis appears to be the number of times that a molecule reverses direction and re-enters the same crystallite. When this is large, the natural draw ratio is large also.

This simple concept accounts successfully for the major features of cold drawing: large differences between different materials, a continuous decrease in the natural draw ratio with the extent of prior extension in the melt, and a decrease in the natural draw ratio on annealing.

#### Acknowledgements

This work was carried out in part while one of the authors (A.N.G.) was a Visiting Scientist at the Institut de Genie des Materiaux, National Research Council of Canada, Boucherville, Quebec. Kind hospitality of the Director, G. Bata, and the Plastics Research Group, led by Professor J.-M. Charrier, is gratefully acknowledged. It forms part of a program of research supported by a grant from the Office of Naval Research (Contract N00014-76-C-0408), and a grant-in-aid from Cabot Corporation.

## References

1. P.I. Vincent, Polymer, 1, 7 (1960).
2. A. Peterlin and H.G. Olf, J. Polym. Sci., Part A-2, 4, 587 (1966).
3. G. Capaccio, T.A. Crompton and I.M. Ward, J. Polym. Sci.: Polym. Phys. Ed., 14, 1461 (1976).
4. L. Mandelkern, Chem. Rev., 56, 903 (1956).
5. A.P. Gray, Thermochim. Acta, 1, 563 (1970).
6. R. Chiang and P.J. Flory, J.Am. Chem. Soc., 83, 2857 (1961).

Table 1. Physical properties of the materials examined

Material	Density $d$ (kg/m <sup>3</sup> )	Crystallinity $C$ (%)	Yield Stress $\sigma_y$ (MPa)	Draw Ratio $\lambda_d$
TPI-X		36*	9.0	2.6
TPI		37*	9.0	2.7
LDPE		50*	10.5	5
MDPE	940	62**	21.5	7
HDPE-1		64*	24	8.6
HDPE-2	955	72**	29	12

\* Measured by DSC with a heating rate of 0.17 C/s.  
 Reported values for 100% crystallinity are: 44.5 cal/g for TPI (4) and 69 cal/g for polyethylene (5).

\*\* C was calculated from the measured density using a relation given by Chiang and Flory (6).

Table 2. Natural draw ratio  $\lambda_d$  for quenched and annealed samples.

Crystallization temperature, $T_c$ (°C)	$\lambda_d$
	TPI-X
0	2.6
40	2.4
45	2.1
	LDPE
Quenched ( $T_c = 20-90$ °C)	4.8
100	5.3
	MDPE
Quenched ( $T_c = 20-100$ °C)	6.4
118	7.7
	HDPE-1
Quenched ( $T_c = 20-100$ °C)	8.6
115	7.0
121	3.5
	HDPE-2
Quenched ( $T_c = 20-100$ °C)	10.5
115	11.0
121	3.0

Figure Legends

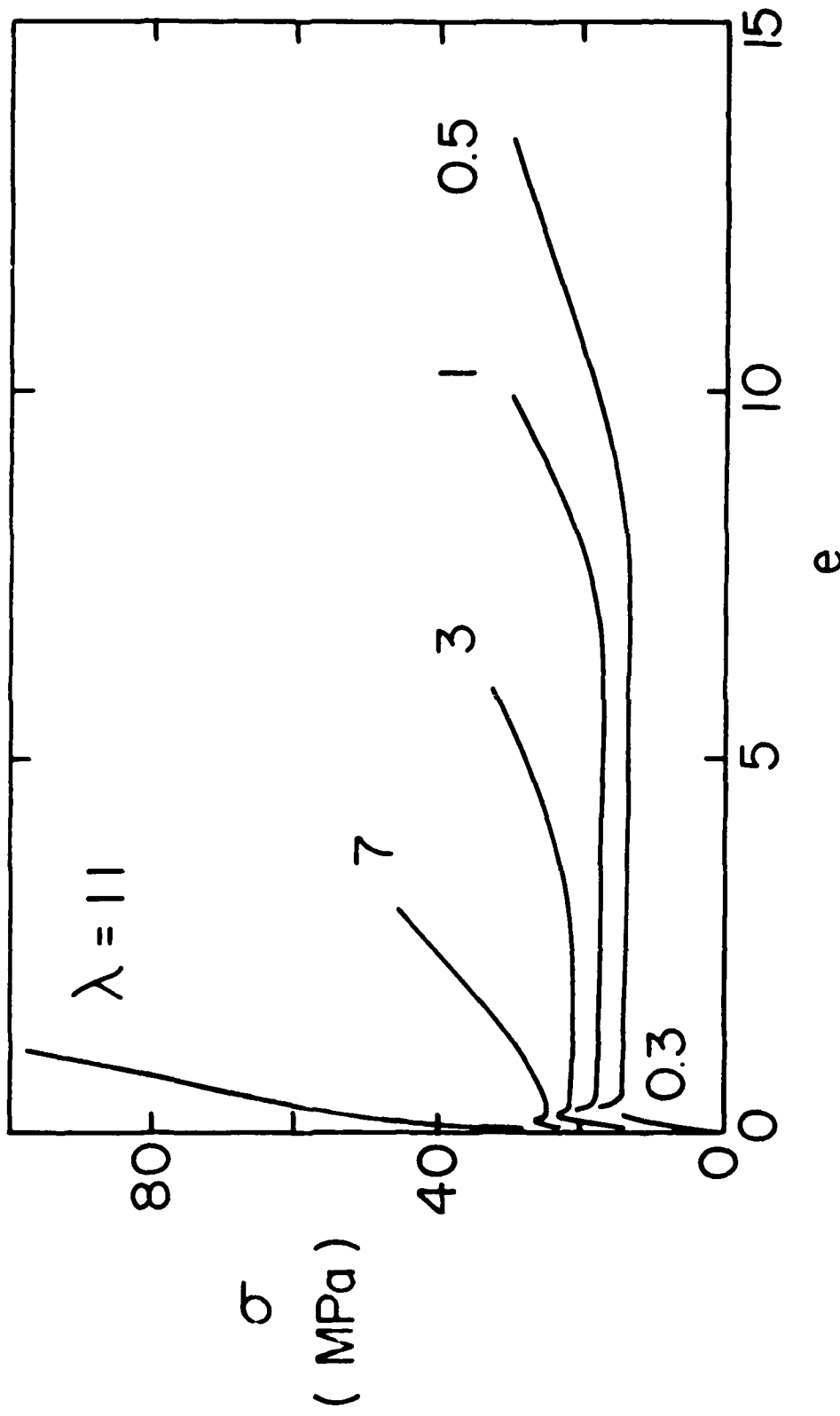
Figure 1. Relations between tensile stress  $\sigma$  and apparent extension  $e$  for oriented samples of HDPE-1.

Figure 2. Relations between tensile stress  $\sigma$  and apparent extension  $e$  for oriented samples of TPI-X.

Figure 3. Dependence of yield stress  $\sigma_y$  upon the prior orientation extension ratio  $\lambda$  in the stretching direction, for HDPE-1, ●, and TPI-X, ○.

Figure 4. Dependence of natural draw ratio  $\lambda_d$  upon the prior orientation extension ratio  $\lambda$  in the stretching direction, for HDPE-1, ●, and TPI-X, ○. The broken lines are drawn with a slope of -1.

Figure 5. (a) Sketch of a molecular strand between tie points in the melt.  
(b) In the crystalline state.  
(c) In the drawn state.

Figure 1

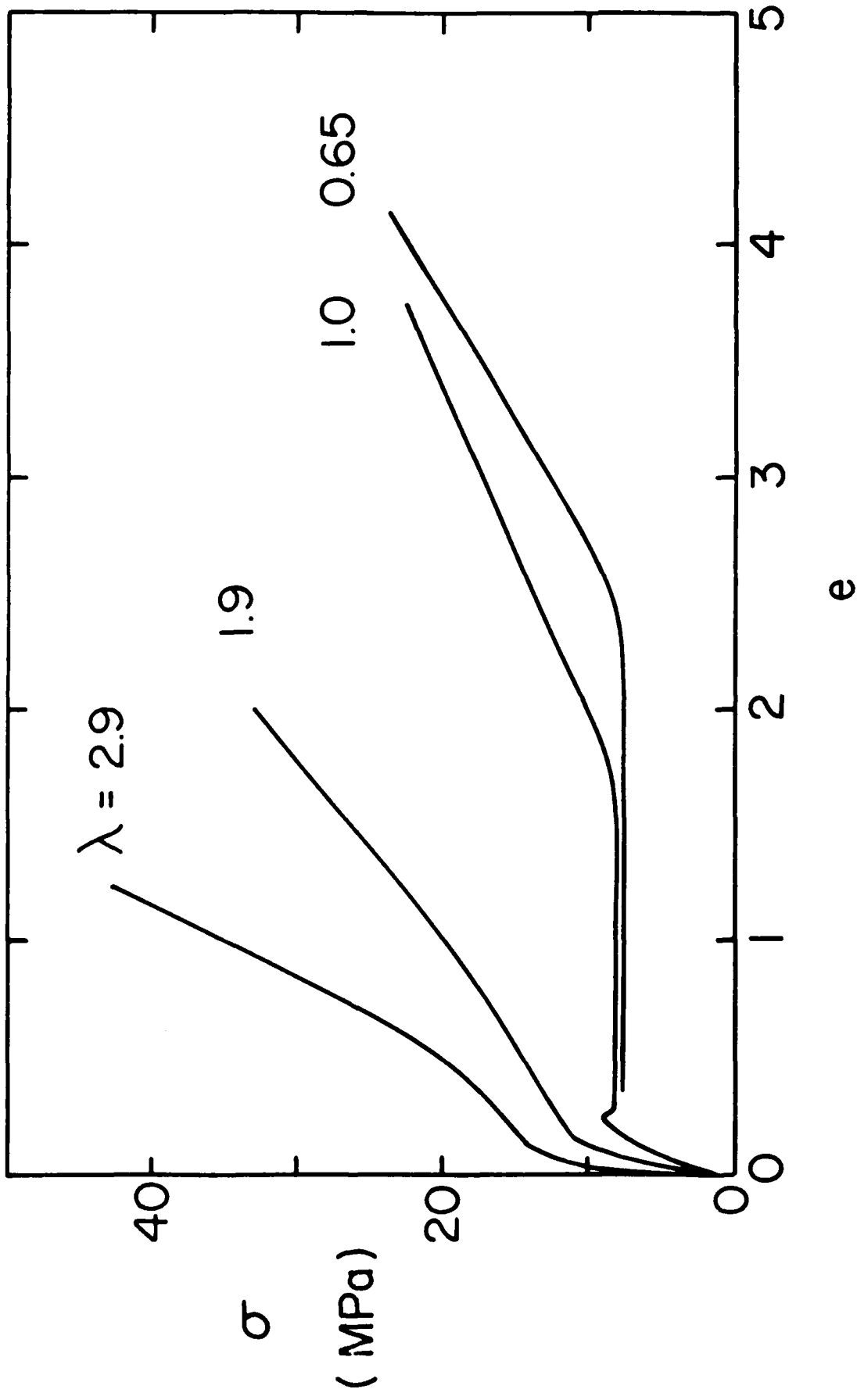


Figure 2

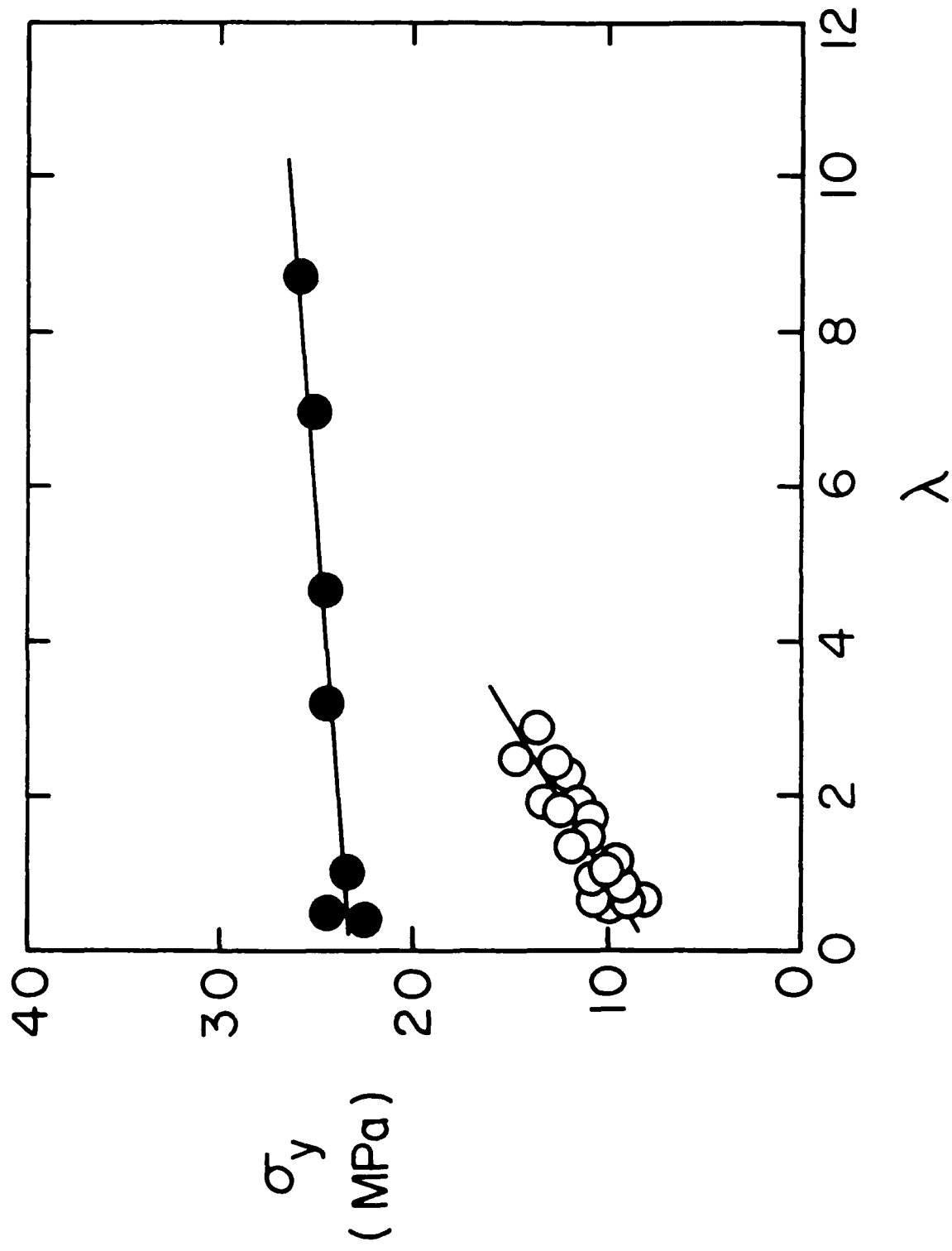


Figure 3

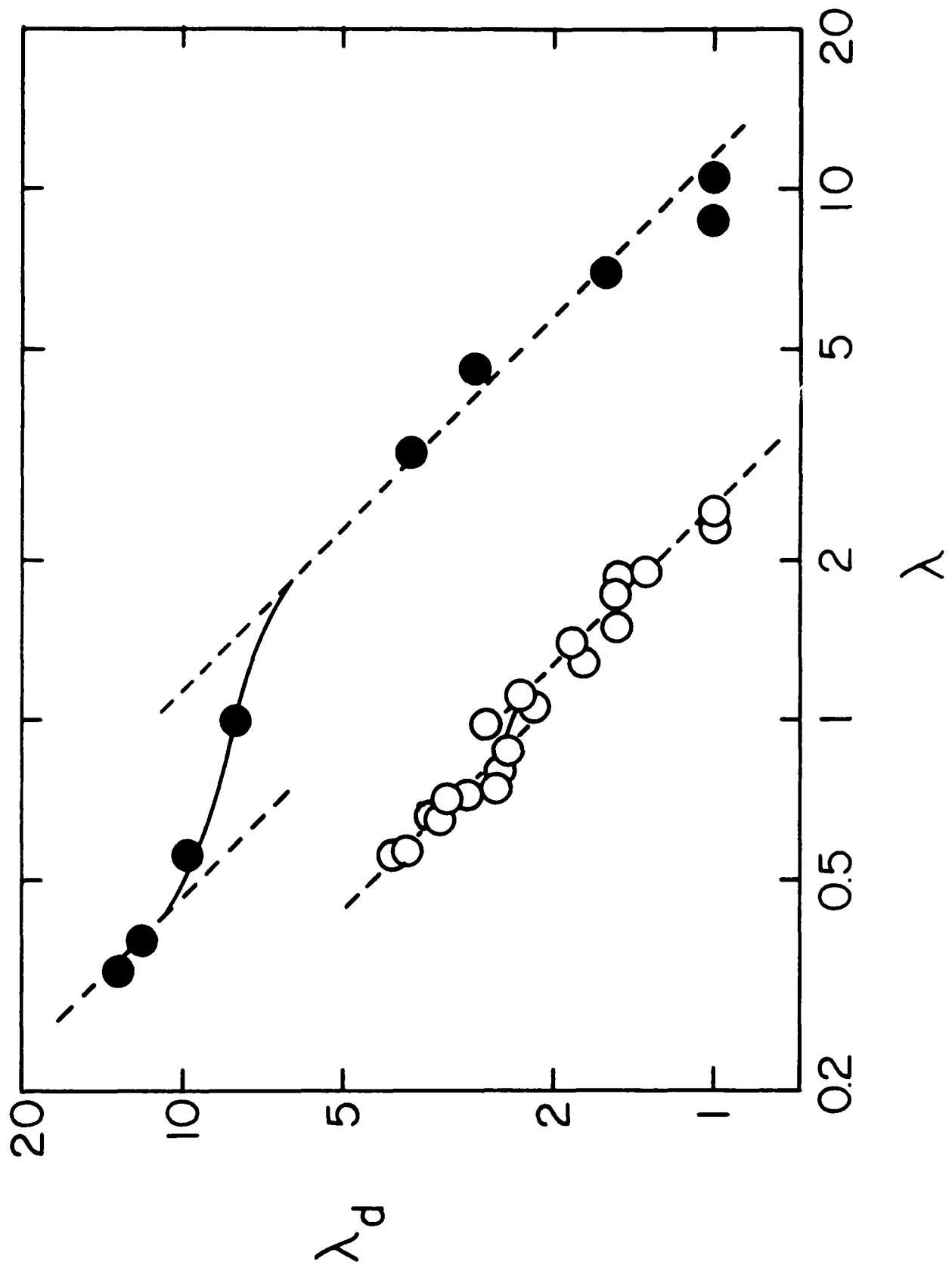


Figure 4

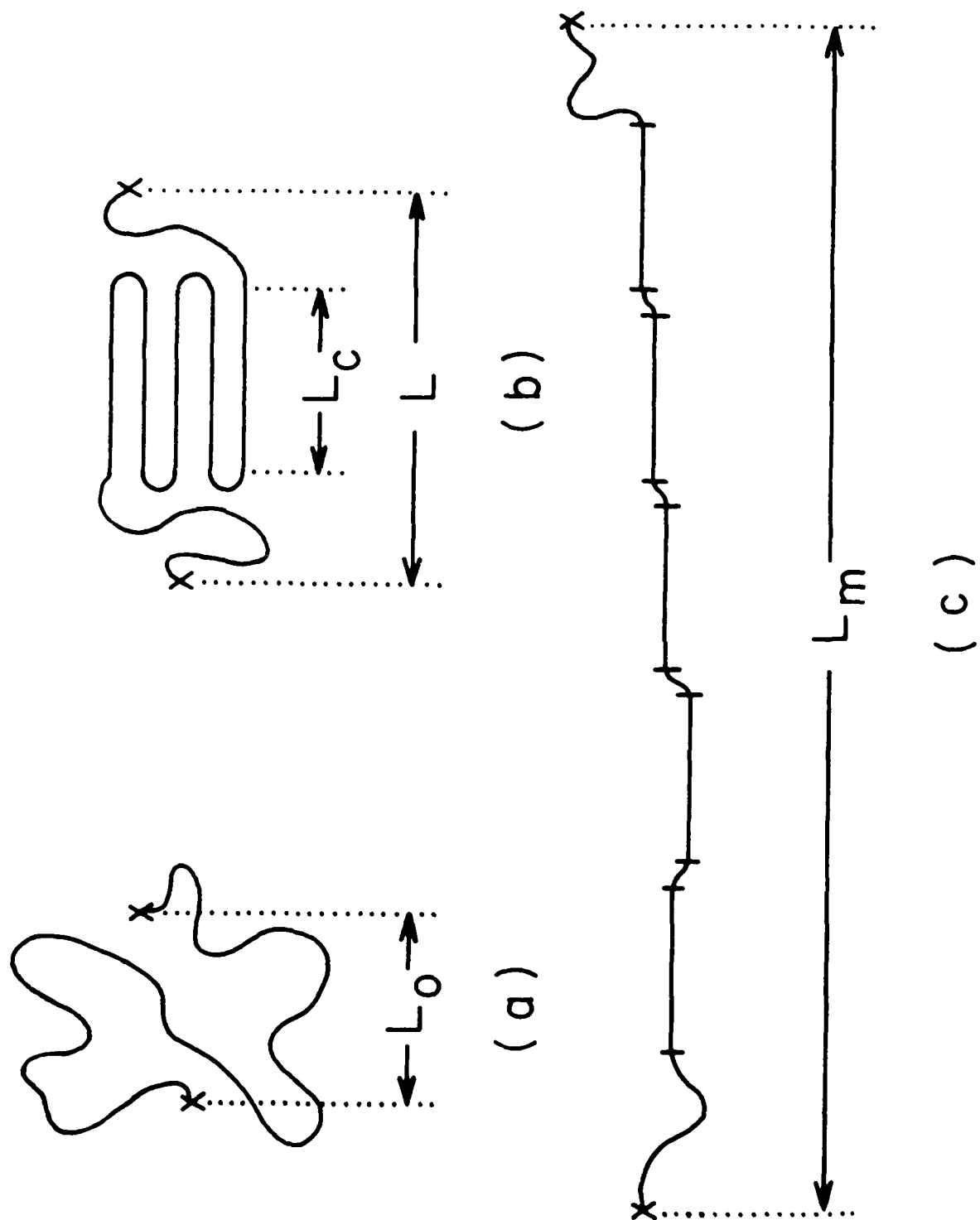


Figure 5

(DYN)

DISTRIBUTION LIST

Dr. R.S. Miller  
Office of Naval Research  
Code 432P  
Arlington, VA 22217  
(10 copies)

Dr. J. Pastine  
Naval Sea Systems Command  
Code 06R  
Washington, DC 20362

Dr. Kenneth D. Hartman  
Hercules Aerospace Division  
Hercules Incorporated  
Alleghany Ballistic Lab  
P.O. Box 210  
Washington, DC 21502

Mr. Otto K. Heiney  
AFATL-DLJC  
Elgin AFB, FL 32542

Dr. Merrill K. King  
Atlantic Research Corp.  
5390 Cherokee Avenue  
Alexandria, VA 22312

Dr. R.L. Lou  
Aerojet Strategic Propulsion Co.  
Bldg. 05025 - Dept 5400 - MS 167  
P.O. Box 15699C  
Sacramento, CA 95813

Dr. R. Olsen  
Aerojet Strategic Propulsion Co.  
Bldg. 05025 - Dept 5400 - MS 167  
P.O. Box 15699C  
Sacramento, CA 95813

Dr. Randy Peters  
Aerojet Strategic Propulsion Co.  
Bldg. 05025 - Dept 5400 - MS 167  
P.O. Box 15699C  
Sacramento, CA 95813

Dr. D. Mann  
U.S. Army Research Office  
Engineering Division  
Box 12211  
Research Triangle Park, NC 27709-2211

Dr. L.V. Schmidt  
Office of Naval Technology  
Code 07CT  
Arlington, VA 22217

JHU Applied Physics Laboratory  
ATTN: CPIA (Mr. T.W. Christian)  
Johns Hopkins Rd.  
Laurel, MD 20707

Dr. R. McGuire  
Lawrence Livermore Laboratory  
University of California  
Code L-324  
Livermore, CA 94550

P.A. Miller  
736 Leavenworth Street, #6  
San Francisco, CA 94109

Dr. W. Moniz  
Naval Research Lab.  
Code 6120  
Washington, DC 20375

Dr. K.F. Mueller  
Naval Surface Weapons Center  
Code R11  
White Oak  
Silver Spring, MD 20910

Prof. M. Nicol  
Dept. of Chemistry & Biochemistry  
University of California  
Los Angeles, CA 90024

Mr. L. Roslund  
Naval Surface Weapons Center  
Code R10C  
White Oak, Silver Spring, MD 20910

Dr. David C. Sayles  
Ballistic Missile Defense  
Advanced Technology Center  
P.O. Box 1500  
Huntsville, AL 35807

(DYN)

DISTRIBUTION LIST

Mr. R. Geisler  
ATTN: DY/MS-24  
AFRPL  
Edwards AFB, CA 93523

Naval Air Systems Command  
ATTN: Mr. Bertram P. Sobers  
NAVAIR-320G  
Jefferson Plaza 1, RM 472  
Washington, DC 20361

R.B. Steele  
Aerojet Strategic Propulsion Co.  
P.O. Box 15699C  
Sacramento, CA 95813

Mr. M. Stasz  
Naval Surface Weapons Center  
Code R10B  
White Oak  
Silver Spring, MD 20910

Mr. E.S. Sutton  
Thiokol Corporation  
Elkton Division  
P.O. Box 241  
Elkton, MD 21921

Dr. Grant Thompson  
Morton Thiokol, Inc.  
Wasatch Division  
MS 240 P.O. Box 524  
Brigham City, UT 84302

Dr. R.S. Valentini  
United Technologies Chemical Systems  
P.O. Box 50015  
San Jose, CA 95150-0015

Dr. R.F. Walker  
Chief, Energetic Materials Division  
DRSMC-LCE (D), B-3022  
USA ARDC  
Dover, NJ 07801

Dr. Janet Wall  
Code 012  
Director, Research Administration  
Naval Postgraduate School  
Monterey, CA 93943

Director  
US Army Ballistic Research Lab.  
ATTN: DRXBR-IBD  
Aberdeen Proving Ground, MD 21005

Commander  
US Army Missile Command  
ATTN: DRSMI-RKL  
Walter W. Wharton  
Redstone Arsenal, AL 35898

Dr. Ingo W. May  
Army Ballistic Research Lab.  
ARRADCOM  
Code DRXBR - IBD  
Aberdeen Proving Ground, MD 21005

Dr. E. Zimet  
Office of Naval Technology  
Code 071  
Arlington, VA 22217

Dr. Ronald L. Derr  
Naval Weapons Center  
Code 389  
China Lake, CA 93555

T. Boggs  
Naval Weapons Center  
Code 389  
China Lake, CA 93555

Lee C. Estabrook, P.E.  
Morton Thiokol, Inc.  
P.O. Box 30058  
Shreveport, Louisiana 71130

Dr. J.R. West  
Morton Thiokol, Inc.  
P.O. Box 30058  
Shreveport, Louisiana 71130

Dr. D.D. Dillehay  
Morton Thiokol, Inc.  
Longhorn Division  
Marshall, TX 75670

G.T. Bowman  
Atlantic Research Corp.  
7511 Wellington Road  
Gainesville, VA 22065

(DYN)

DISTRIBUTION LIST

R.E. Shenton  
Atlantic Research Corp.  
7511 Wellington Road  
Gainesville, VA 22065

Mike Barnes  
Atlantic Research Corp.  
7511 Wellington Road  
Gainesville, VA 22065

Dr. Lionel Dickinson  
Naval Explosive Ordnance  
Disposal Tech. Center  
Code D  
Indian Head, MD 20340

Prof. J.T. Dickinson  
Washington State University  
Dept. of Physics 4  
Pullman, WA 99164-2814

M.H. Miles  
Dept. of Physics  
Washington State University  
Pullman, WA 99164-2814

Dr. T.F. Davidson  
Vice President, Technical  
Morton Thiokol, Inc.  
Aerospace Group  
110 North Wacker Drive  
Chicago, Illinois 60606

Mr. J. Consaga  
Naval Surface Weapons Center  
Code R-16  
Indian Head, MD 20640

Naval Sea Systems Command  
ATTN: Mr. Charles M. Christensen  
NAVSEA-62R2  
Crystal Plaza, Bldg. 6, Rm 806  
Washington, DC 20362

Mr. R. Beauregard  
Naval Sea Systems Command  
SEA 64E  
Washington, DC 20362

Brian Wheatley  
Atlantic Research Corp.  
7511 Wellington Road  
Gainesville, VA 22065

Mr. G. Edwards  
Naval Sea Systems Command  
Code 62R32  
Washington, DC 20362

C. Dickinson  
Naval Surface Weapons Center  
White Oak, Code R-13  
Silver Spring, MD 20910

Prof. John Deutch  
MIT  
Department of Chemistry  
Cambridge, MA 02139

Dr. E.H. deButts  
Hercules Aerospace Co.  
P.O. Box 27408  
Salt Lake City, UT 84127

David A. Flanigan  
Director, Advanced Technology  
Morton Thiokol, Inc.  
Aerospace Group  
110 North Wacker Drive  
Chicago, Illinois 60606

Dr. L.H. Caveny  
Air Force Office of Scientific  
Research  
Directorate of Aerospace Sciences  
Bolling Air Force Base  
Washington, DC 20332

W.G. Roger  
Code 5253  
Naval Ordnance Station  
Indian Head, MD 20640

Dr. Donald L. Ball  
Air Force Office of Scientific  
Research  
Directorate of Chemical &  
Atmospheric Sciences  
Bolling Air Force Base  
Washington, DC 20332

(DYN)

DISTRIBUTION LIST

Dr. Anthony J. Matuszko  
Air Force Office of Scientific Research  
Directorate of Chemical & Atmospheric  
Sciences  
Bolling Air Force Base  
Washington, DC 20332

Dr. Michael Chaykovsky  
Naval Surface Weapons Center  
Code R11  
White Oak  
Silver Spring, MD 20910

J.J. Rocchio  
USA Ballistic Research Lab.  
Aberdeen Proving Ground, MD 21005-5066

G.A. Zimmerman  
Aerojet Tactical Systems  
P.O. Box 13400  
Sacramento, CA 95813

B. Swanson  
INC-4 MS C-346  
Los Alamos National Laboratory  
Los Alamos, New Mexico 87545

Dr. James T. Bryant  
Naval Weapons Center  
Code 3205B  
China Lake, CA 93555

Dr. L. Rothstein  
Assistant Director  
Naval Explosives Dev. Engineering Dept.  
Naval Weapons Station  
Yorktown, VA 23691

Dr. M.J. Kamlet  
Naval Surface Weapons Center  
Code R11  
White Oak, Silver Spring, MD 20910

Dr. Henry Webster, III  
Manager, Chemical Sciences Branch  
ATTN: Code 5063  
Crane, IN 47522

Dr. A.L. Slafkosky  
Scientific Advisor  
Commandant of the Marine Corps  
Code RD-1  
Washington, DC 20380

Dr. H.G. Adolph  
Naval Surface Weapons Center  
Code R11  
White Oak  
Silver Spring, MD 20910

U.S. Army Research Office  
Chemical & Biological Sciences  
Division  
P.O. Box 12211  
Research Triangle Park, NC 27709

G. Butcher  
Hercules, Inc.  
MS X2H  
P.O. Box 98  
Magna, Utah 84044

W. Waesche  
Atlantic Research Corp.  
7511 Wellington Road  
Gainesville, VA 22065

Dr. John S. Wilkes, Jr.  
FJSRL/NC  
USAF Academy, CO 80840

Dr. H. Rosenwasser  
AIR-320R  
Naval Air Systems Command  
Washington, DC 20361

Dr. Joyce J. Kaufman  
The Johns Hopkins University  
Department of Chemistry  
Baltimore, MD 21218

Dr. A. Nielsen  
Naval Weapons Center  
Code 385  
China Lake, CA 93555

(DYN)

DISTRIBUTION LIST

K.D. Pae  
High Pressure Materials Research Lab.  
Rutgers University  
P.O. Box 909  
Piscataway, NJ 08854

Dr. John K. Dienes  
T-3, B216  
Los Alamos National Lab.  
P.O. Box 1663  
Los Alamos, NM 87544

A.N. Gent  
Institute Polymer Science  
University of Akron  
Akron, OH 44325

Dr. D.A. Shockey  
SRI International  
333 Ravenswood Ave.  
Menlo Park, CA 94025

Dr. R.B. Kruse  
Mercon Thickol, Inc.  
Huntsville Division  
Huntsville, AL 35807-7501

G. Butcher  
Hercules, Inc.  
P.O. Box 98  
Magna, UT 84044

W. Waesche  
Atlantic Research Corp.  
7511 Wellington Road  
Gainesville, VA 22065

Dr. R. Bernecker  
Naval Surface Weapons Center  
Code R13  
White Oak  
Silver Spring, MD 20910

Prof. Edward Price  
Georgia Institute of Tech.  
School of Aerospace Engineering  
Atlanta, GA 30332

J.A. Birkett  
Naval Ordnance Station  
Code 5253K  
Indian Head, MD 20640

Prof. R.W. Armstrong  
University of Maryland  
Dept. of Mechanical Engineering  
College Park, MD 20742

Herb Richter  
Code 385  
Naval Weapons Center  
China Lake, CA 93555

J.T. Rosenberg  
SRI International  
333 Ravenswood Ave.  
Menlo Park, CA 94025

G.A. Zimmerman  
Aeroject Tactical Systems  
P.O. Box 13400  
Sacramento, CA 95813

Prof. Kenneth Kuo  
Pennsylvania State University  
Dept. of Mechanical Engineering  
University Park, PA 16802

T.L. Boggs  
Naval Weapons Center  
Code 3891  
China Lake, CA 93555

(DYN)

DISTRIBUTION LIST

Dr. C.S. Coffey  
Naval Surface Weapons Center  
Code R13  
White Oak  
Silver Spring, MD 20910

D. Curran  
SRI International  
333 Ravenswood Avenue  
Menlo Park, CA 94025

E.L. Throckmorton  
Code SP-2731  
Strategic Systems Program Office  
Crystal Mall #3, RM 1048  
Washington, DC 23076

Dr. R. Martinson  
Lockheed Missiles and Space Co.  
Research and Development  
3251 Hanover Street  
Palo Alto, CA 94304

C. Gotzmer  
Naval Surface Weapons Center  
Code R-11  
White Oak  
Silver Spring, MD 20910

G.A. Lo  
3251 Hanover Street  
B204 Lockheed Palo Alto Research Lab  
Palo Alto, CA 94304

R.A. Schapery  
Civil Engineering Department  
Texas A&M University  
College Station, TX 77843

J.M. Culver  
Strategic Systems Projects Office  
SSPO/SP-2731  
Crystal Mall #3, RM 1048  
Washington, DC 20376

Prof. G.D. Duvall  
Washington State University  
Department of Physics  
Pullman, WA 99163

Dr. E. Martin  
Naval Weapons Center  
Code 3858  
China Lake, CA 93555

Dr. M. Farber  
135 W. Maple Avenue  
Monrovia, CA 91016

W.L. Elban  
Naval Surface Weapons Center  
White Oak, Bldg. 343  
Silver Spring, MD 20910

G.E. Manser  
Morton Thiokol  
Wasatch Division  
P.O. Box 524  
Brigham City, UT 84302

R.G. Rosemeier  
Brimrose Corporation  
7720 Belair Road  
Baltimore, MD 20742

Ser 432/84/340  
Revised January 1985

Administrative Contracting  
Officer (see contract for  
address)  
(1 copy)

Director  
Naval Research Laboratory  
Attn: Code 2627  
Washington, DC 20375  
(6 copies)

Defense Technical Information Center  
Bldg. 5, Cameron Station  
Alexandria, VA 22314  
(12 copies)

Dr. Robert Polvani  
National Bureau of Standards  
Metallurgy Division  
Washington, D.C. 20234

Dr. Y. Gupta  
Washington State University  
Department of Physics  
Pullman, WA 99163

**END**

**FILMED**

**4-85**

**DTIC**

